A Wideband Dual-Polarized Omnidirectional Antenna for Base Station/WLAN

Jun Wang, Lei Zhao, *Member, IEEE*, Zhang-Cheng Hao, *Senior Member, IEEE*, and Jian-Ming Jin, *Fellow, IEEE*

***Abstract*— A wideband dual-polarized omnidirectional antenna is proposed for mobile communication base station and 2.4 GHz wireless local area network applications. An integrated design is achieved by combining an inverted-cone monopole for vertical polarization (VP) and a modified cross bow-tie dipole for horizontal polarization (HP). The proposed antenna has a compact size because the HP element acts as the HP radiating element and the ground plane for the VP element simultaneously. The proposed VP and HP antennas are excited by a 50 Ω Sub-Miniature-A connector and a broadband feeding network, respectively. The overall volume of the proposed antenna is only $0.35\lambda_0 \times 0.35\lambda_0 \times 0.25\lambda_0$ (with λ_0 being the wavelength of the lowest frequency). Simulation results show that the dual-polarized omnidirectional antenna achieves a bandwidth (for $|S_{11}| < -10$ dB) of about 41.5% (1.64–2.5 GHz) with an isolation of at least 25 dB and the gain variations at the center frequency in the horizontal plane are 0.7 dB for VP and 2.3 dB for HP. The good agreements between the simulation and measured results validate the proposed design.**

***Index Terms*— Dual-polarized omnidirectional antenna, inverted-cone monopole, modified cross bow-tie dipole.**

I. Introduction

OMNIDIRECTIONAL antennas have received a great deal of attention for wireless communication systems, such as base stations [1], [2], wireless local area networks (WLANs) [3], and many portable devices [4]. For modern base station/WLAN systems, compact wideband dual-polarized omnidirectional antennas are necessary components. However, designing such antennas is technically very challenging.

According to the open literature, the most effective approach to achieve dual polarizations is to combine different vertical polarization (VP) or horizontal polarization (HP) antennas. The coaxial collinear antenna [5] and inverted hat [6] were widely used for achieving a VP, while the loop antenna [3] and planar folded dipole [7] were proposed for realizing an HP. In practical applications, it is of great importance to seek a compact design for a wideband dual-polarization antenna with a good isolation. Recently, several designs were proposed to achieve dual polarizations [8]–[16]. In [8], a compact omnidirectional dual-polarized antenna using highly isolated slots was designed for 2.4 GHz WLAN, achieving an operating bandwidth of 9.5%. Another dual-polarized omnidirectional planar slot antenna was presented in [9] for 5.2 GHz WLAN, with a bandwidth of about 10% and different omnidirectional planes for VP and HP. To enhance the bandwidth, some novel antenna designs for mobile communications systems were proposed in [12]–[14]. Specifically, a combination of a modified low-profile monopole and a planar circular loop was proposed in [12]. A design composing of four vertical dipoles and four horizontal dipoles was presented in [13]. Furthermore, a center-fed discone combined with a printed dipole array was designed for bandwidth enhancement [14]. In [15], an artificial magnetic conductor reflector was applied to reduce the profile height of the designed wideband dual-polarized antenna. A wideband dual-polarized antenna for spectrum monitoring systems was proposed in [16] by merging an inverted-cone monopole and a cross bow-tie. However, its radiation patterns have to be improved to serve as an omnidirectional antenna.

In this paper, a new wideband dual-polarized omnidirectional antenna, similar to the one in [16], is proposed for base station/WLAN systems. The antenna employs an inverted-cone monopole for the VP and an interconnected cross bow-tie as the HP element for improving the impedance matching and the omnidirectional radiation pattern in the *xy* plane. The proposed antenna has the following improvements compared to the previous work in [16].

1) The input impedance of the HP element is decreased from 200 to 50 Ω by using the shorting pins.
2) The stability of the omnidirectional radiation patterns in the *xy* plane over all the frequency bands is improved effectively.
3) The HP omnidirectional pattern is further analyzed using mathematical formulas.
4) The omnidirectional frequency band covers 1.64–2.5 GHz, which enables the simultaneous use for mobile communication base station and 2.4 GHz WLAN applications.

Manuscript received July 18, 2017; revised October 12, 2017; accepted November 6, 2017. Date of publication November 10, 2017; date of current version January 2, 2018. This work was supported in part by the National Science Foundation of China under Grant 61771226, Grant 61372057, and Grant 61671223, and in part by the Open Project of State Key Laboratory of Millimeter Waves under Grant K201613. *(Corresponding author: Lei Zhao; Zhang-Cheng Hao.)*

J. Wang and L. Zhao are with the Center for Computational Science and Engineering, Jiangsu Normal University, Xuzhou 221116, China, and also with the State Key Laboratory of Millimeter Waves, School of Information Science and Engineering, Southeast University, Nanjing 210096, China (e-mail: xzjwang@163.com; leizhao@jsnu.edu.cn).

Z.-C. Hao is with the State Key Laboratory of Millimeter Waves, School of Information Science and Engineering, Southeast University, Nanjing 210096, China (e-mail: zchao@seu.edu.cn).

J.-M. Jin is with the Department of Electrical and Computer Engineering, University of Illinois at Urbana-Champaign, Urbana, IL 61801 USA (e-mail: j-jin1@illinois.edu).

Color versions of one or more of the figures in this paper are available online at http://ieeexplore.ieee.org.

Digital Object Identifier 10.1109/TAP.2017.2772322

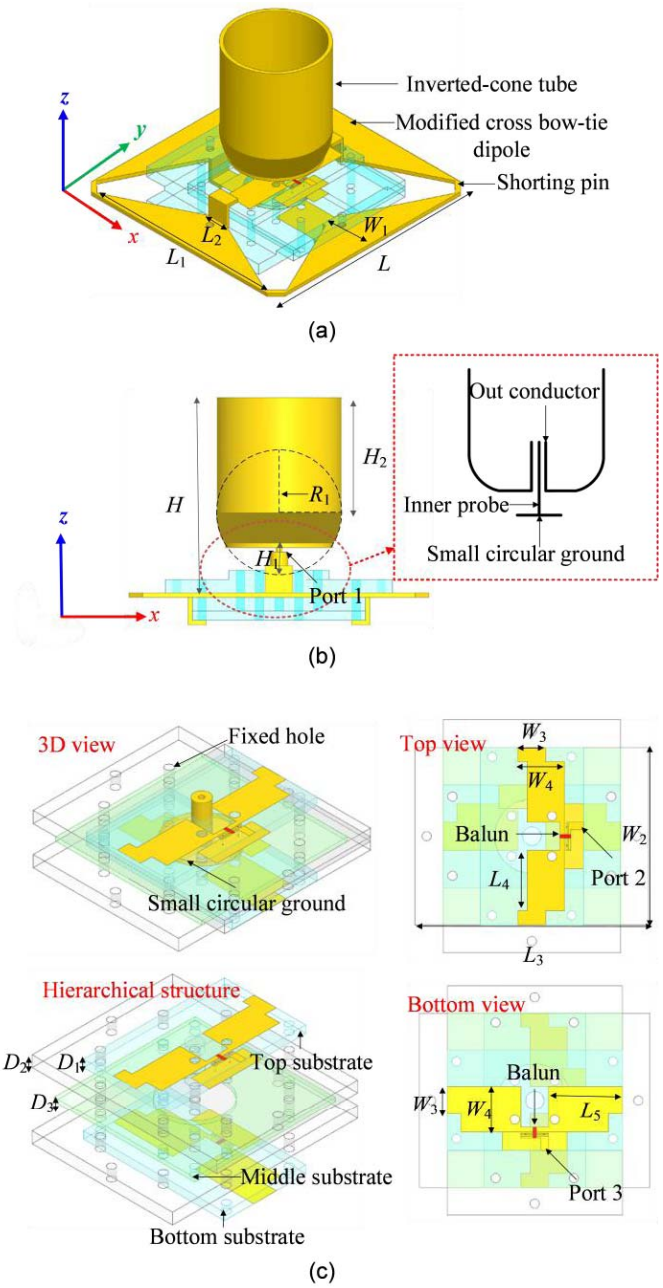

Fig. 1. (a) Simulated model of the wideband dual-polarized omnidirectional antenna. (b) Side view and the structure of the SMA connection of VP element. (c) Feeding structure of the HP element (L = 66 mm, L_1 = 60 mm, L_2 = 6 mm, L_3 = 50 mm, L_4 = 13 mm, L_5 = 16 mm, W_1 = 13 mm, W_2 = 38 mm, W_3 = 6 mm, W_4 = 10 mm, R = 8 mm, R_1 = 12.7 mm, H = 43.1 mm, H_1 = 6 mm, H_2 = 25.4 mm, D_1 = 2 mm, D_2 = 3 mm, and D_3 = 1 mm).

II. Antenna Configuration

The configuration of the proposed wideband dual-polarized omnidirectional antenna is sketched in Fig. 1, which is a combination of an element for VP and an element for HP. The VP element is mainly an inverted-cone monopole, and the HP element is a modified cross bow-tie dipole. The two elements are integrated in a compact size by using a small circular ground, which is located at the middle position of the HP element. Fig. 1(a)–(c) shows the entire model of the proposed antenna, the side view and Sub-Miniature-A (SMA) connection schematic for the VP antenna, and the feeding structure of the whole antenna, respectively, where L denotes the base dimension of the proposed antenna.

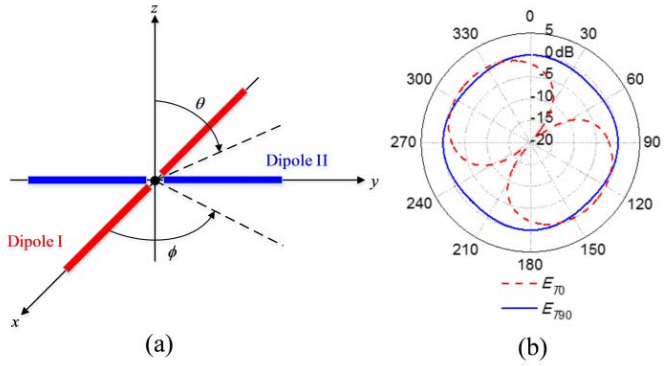

Fig. 2. Geometry and normalized radiation pattern of a cross dipole of finite length in the xy plane. (a) Cross dipole. (b) E_{T0} and E_{T90} when $l = 0.25\ \lambda_c$. (λ_c is the wavelength at the center frequency.)

The whole VP element is composed of an inverted-cone tube, a small circular ground of radius R, and a modified cross bow tie. It is excited by an inverted 50 Ω SMA connector, as shown in Fig. 1(b). The inverted-cone tube is composed of a cylindrical tube and a feeding port with a gradually changed radius. The radius of the circularly contoured feeding port surface is denoted by R_1, the height of the cutting-off part is denoted by H_1, and the height of the cylindrical tube is H_2.

The HP element is made of an interconnected cross bow-tie dipole and optimized feeding striplines printed on the FR4 substrates. The top and bottom striplines are set to be different to allow for model optimization. A commercial RF balun is used to connect each of the striplines. As shown in Fig. 1(a) and (c), the sizes of the bow-tie arms are denoted by L_1, L_2, and W_1. The dimension of the substrates and feeding striplines are W_2, W_3, W_4, L_3, L_4, and L_5, respectively. The thicknesses of the substrates are denoted by D_1, D_2, and D_3, respectively.

III. Design Considerations

A. Antenna Operating Principle

The proposed design combines a VP element and an HP element. The radius and height of the VP element determine its lowest working frequency. The vertically polarized radiation is produced by the outward traveling waves. To generate an omnidirectional HP radiation, the HP element is designed and fed by a broadband feeding network that produces two outputs of the same amplitude with a 90° phase difference to rotate the electric field [17].

To illustrate how to achieve an HP omnidirectional pattern in the xy plane, let us consider a finite-length cross dipole antenna, as shown in Fig. 2(a). Assume that the amplitudes of the currents on the dipoles (I and II) are I_1 and I_2, respectively. Accordingly, the electric fields of dipoles I and II [18] in the

xy plane can be expressed as

$$\vec{E}_{I}(r,\phi,\pi/2) = \hat{\phi}\, j I_1 \eta \frac{\cos(kl\cos\phi) - \cos kl}{\sin\phi} \frac{e^{-jkr}}{2\pi r} \quad (1)$$

$$\vec{E}_{II}(r,\phi,\pi/2) = -\hat{\phi}\, j I_2 \eta \frac{\cos(kl\sin\phi) - \cos kl}{\cos\phi} \frac{e^{-jkr}}{2\pi r} \quad (2)$$

where η, k, and l are the free-space intrinsic impedance, the free-space wavenumber, and the length of the cross dipole arm, respectively. Then, the total electric field of the cross dipole under the excitations with the same amplitude ($I_1 = I_2 = I$) and a phase difference of 0° ($\vec{E}_{T0}$) or 90° ($\vec{E}_{T90}$) can be obtained as

$$\begin{aligned}\vec{E}_{T0}(r,\phi,\pi/2) &= \vec{E}_{I}(r,\phi,\pi/2) + \vec{E}_{II}(r,\phi,\pi/2) \\ &= \hat{\phi}\, j I \eta \left\{ \frac{\cos(kl\cos\phi) - \cos kl}{\sin\phi} \right. \\ &\quad \left. - \frac{\cos(kl\sin\phi) - \cos kl}{\cos\phi} \right\} \frac{e^{-jkr}}{2\pi r} \end{aligned} \quad (3)$$

$$\begin{aligned}\vec{E}_{T90}(r,\phi,\pi/2) &= \vec{E}_{I}(r,\phi,\pi/2) + j\vec{E}_{II}(r,\phi,\pi/2) \\ &= \hat{\phi} I \eta \left\{ \frac{\cos(kl\sin\phi) - \cos kl}{\cos\phi} \right. \\ &\quad \left. + j\frac{\cos(kl\cos\phi) - \cos kl}{\sin\phi} \right\} \frac{e^{-jkr}}{2\pi r}. \end{aligned} \quad (4)$$

The normalized $\vec{E}_{T0}$ and $\vec{E}_{T90}$ patterns of the cross dipole in the *xy* plane are plotted in Fig. 2(b), which shows that the cross dipole can produce a good HP omnidirectional radiation in the *xy* plane with the excitations of the same amplitude and a 90° phase difference. Therefore, two orthogonal dipoles are a suitable candidate to produce an omnidirectional HP radiation pattern.

Now consider the functions of the small circular ground. When the VP element is fed, an opposite directed current appears on the HP element by electromagnetic coupling from the small circular ground, which is similar to that on the ground plane of a traditional monopole antenna. However, the small ground has a negative effect on the HP element, because if the distance between the bow-tie arms and the small ground is too small, their coupling becomes too strong such that the HP element will be shorted by the small ground. This problem can be alleviated by selecting a proper distance such that most currents would flow from one arm of the HP element to another arm via the excitation port even though there are still some coupling currents on the small ground. Consequently, the HP element can be regarded as a cross dipole antenna.

The HP element uses four shorting pins to connect the four bow-tie arms to each other. This modification is important because the shorting pins have two functions: 1) to improve the impedance matching and 2) to ameliorate the omnidirectional radiation pattern. Since ports 2 and 3 are nearly symmetrical, only the simulated input impedance of port 2 with and without the shorting pins is shown. As can be observed in Fig. 3(a), the inductive components of the shorting pins can compensate the capacitive components caused by the cross bow-tie dipole to improve the input impedance matching. Moreover, the

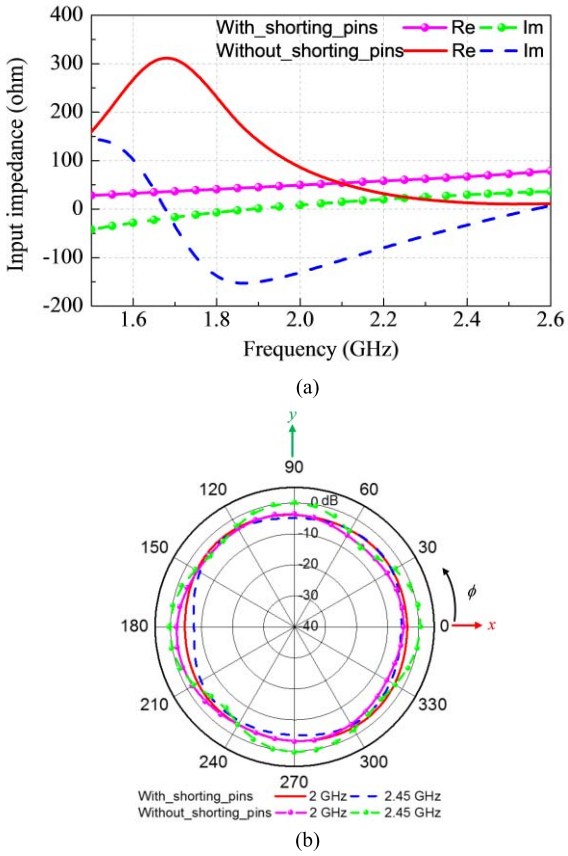

Fig. 3. Simulated input impedance of port 2 and radiation pattern of the HP antenna in the *xy* plane with and without the shorting pins. (a) Input impedance of port 2. (b) Radiation pattern of the HP antenna.

designed shorting pins make the impedance matching close to 50 Ω, which is beneficial to the antenna design and fabrication. Furthermore, Fig. 3(b) shows that the shorting pins can ameliorate the omnidirectional radiation pattern in the *xy* plane effectively. The gain variations are reduced from 4.6 to 2.3 dB at 2 GHz and from 7.5 to 4.6 dB at 2.45 GHz.

B. Antenna Performance

Following the geometrical description and operating principle explained above, the antenna performance is now investigated. It should be mentioned that since HFSS cannot simulate the proposed antenna with commercial RF baluns, the RF baluns need to be assumed as ideal devices and 50 Ω lumped ports with the same amplitude and a 90° phase deviation are used for the HP element excitation.

When the VP element is excited, the simulated reflection coefficient $|S_{11}|$ and gain values of the proposed VP element are plotted in Fig. 4. It is obvious that the VP element can maintain a good impedance matching within a wide frequency range and the 10 dB return loss bandwidth is achieved from 1.6 to 2.6 GHz. Additionally, the simulated radiation patterns of the inverted-cone monopole at 2 and 2.45 GHz are presented in Fig. 5, showing that the gain variations of the inverted-cone monopole in the horizontal plane are 0.7 and 2 dB at 2 and 2.45 GHz, respectively.

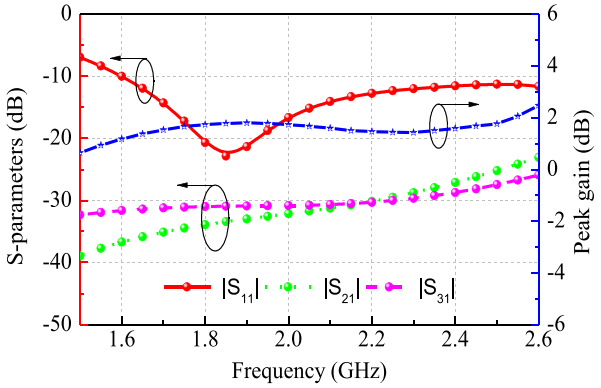

Fig. 4. Simulated $|S_{11}|$ and gain values of the proposed inverted-cone monopole and the mutual coupling between the VP and HP elements.

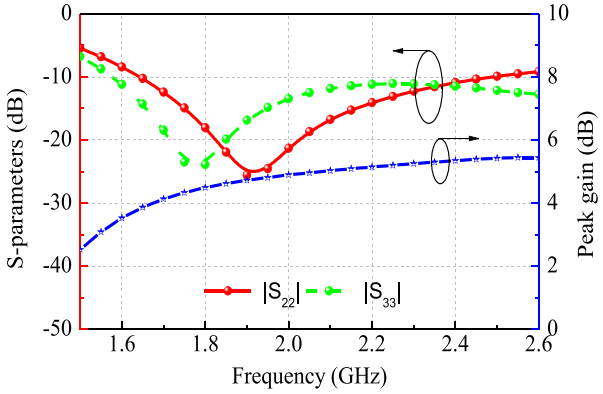

Fig. 6. Simulated $|S_{22}|$, $|S_{33}|$, and gain values of the HP element.

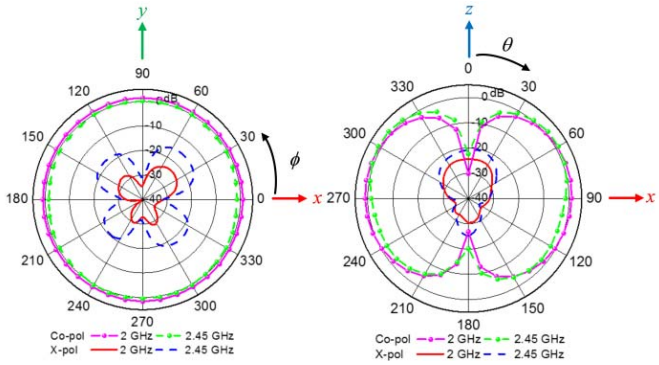

Fig. 5. Simulated radiation patterns of the VP element at 2 and 2.45 GHz.

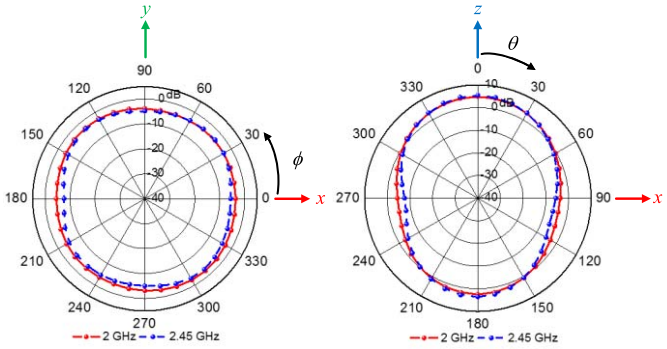

Fig. 7. Simulated radiation patterns of the HP element at 2 and 2.45 GHz with the excitations of the same amplitude and a 90° phase deviation.

When the HP element is excited with the same amplitude and a 90° phase deviation, the horizontally polarized omnidirectional radiation can be obtained and the simulation results are presented in Figs. 6 and 7, respectively. As shown in Fig. 6, the operating frequency ($|S_{22}|$ and $|S_{33}| < -10$ dB) of the modified cross bow-tie dipole is from 1.64 to 2.5 GHz for $|S_{22}|$ and 1.56 to 2.6 GHz for $|S_{33}|$. The $|S_{22}|$ and $|S_{33}|$ of the cross bow-tie dipole are a little different due to the influence of the inverted-cone on the feeding structure of port 2. The simulated gain value is 3.9 dB at 1.64 GHz, which increases to 5.42 dB at 2.5 GHz. For the HP in the *xy* plane, the bandwidth for gain variation less than 4.6 dB is from 1.64 to 2.45 GHz. The radiation patterns at 2 and 2.45 GHz are displayed in Fig. 7, from which good omnidirectional radiation patterns are observed in the *xy* plane.

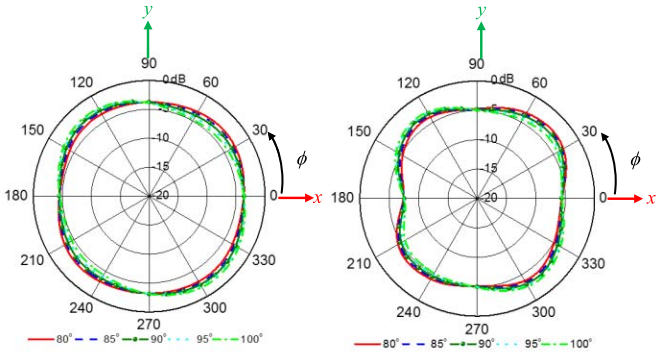

(a) (b)

Fig. 8. Simulated omnidirectional radiation patterns of the HP element under different phase excitations at 2 and 2.45 GHz in the *xy* plane. (a) 2 GHz. (b) 2.45 GHz.

IV. Parametric Study on Phase Difference

The HP element is fed by a 90° feeding network to radiate a horizontally polarized omnidirectional pattern by rotating the electric field, which requires the feeding network to produce two outputs of the same amplitude with a 90° phase difference. Therefore, the phase information plays an important role on the omnidirectional radiation pattern of the modified cross bow-tie dipole. A parametric study is conducted here to analyze the effects of the phase difference on the radiation performance and help to guide the practical design of the proposed modified cross bow-tie dipole.

Fig. 8 shows the simulated omnidirectional radiation patterns of the modified cross bow-tie dipole under excitations with different phase differences at 2 and 2.45 GHz in the *xy* plane. The gain variations are 1.94, 2.3, and 3.1 dB at 2 GHz under the excitation of 80°, 90°, and 100° phase differences, respectively. The gain variations are 5, 4.6, and 5.2 dB at 2.45 GHz under the excitation of 80°, 90°, and 100° phase differences, respectively. This parametric study illustrates that the phase deviation within 10° is an acceptable range, which helps to understand the measured omnidirectional

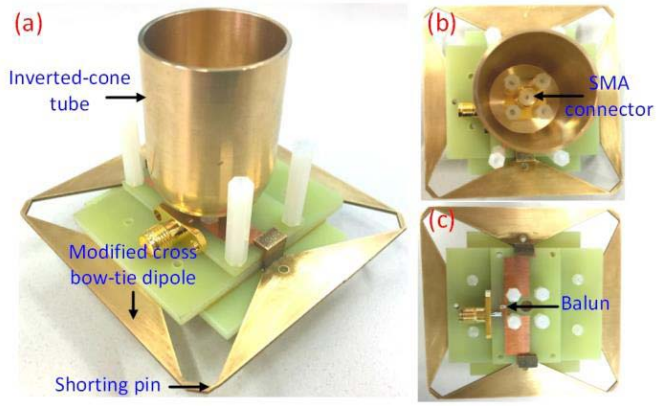

Fig. 9. Photographs of the fabricated antenna. (a) 3-D view. (b) Top view. (c) Bottom view.

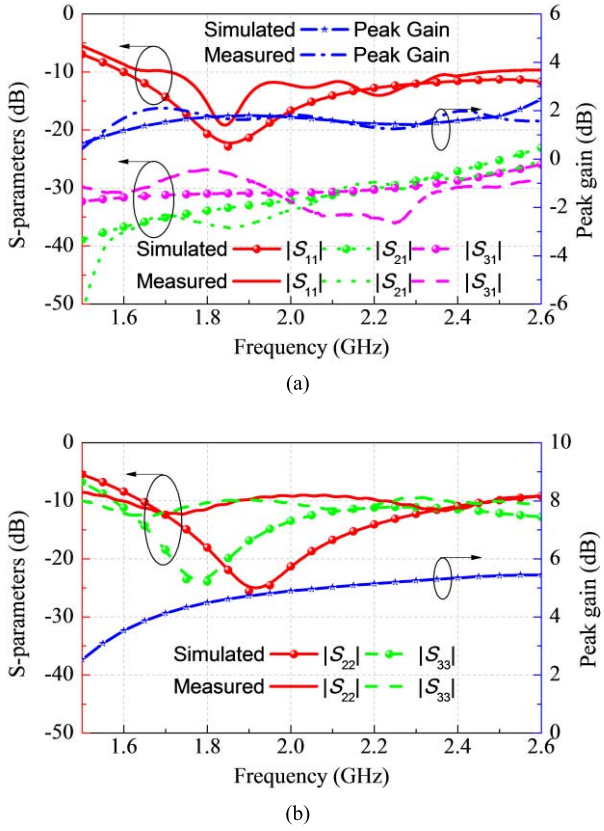

Fig. 10. Simulation and measured results of the proposed antenna. (a) VP element and its mutual coupling with the HP element and (b) HP element.

radiation patterns of the fabricated modified cross bow-tie antenna.

V. Experimental Verification

A prototype of the proposed wideband dual-polarized omnidirectional antenna is fabricated, as show in Fig. 9. The feeding striplines of the HP element are printed on the FR4 substrates (with $\varepsilon_r = 4.4$ and $\tan\delta = 0.002$). Two NCS1-292 RF baluns are soldered on its top and bottom striplines, respectively. Moreover, the outer conductor of a 50 Ω SMA connector is soldered onto the inverted-cone tube and the inner conductor is connected to the small circular ground.

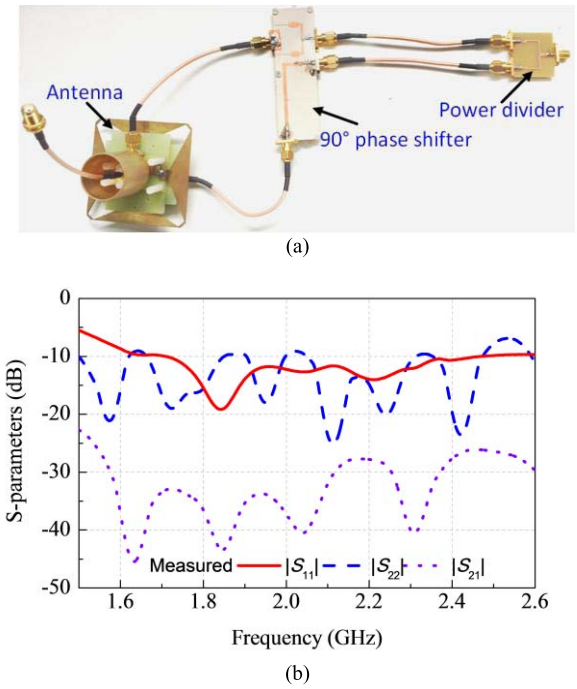

Fig. 11. (a) Configuration and (b) measured S-parameters of the proposed antenna combined with a feeding network.

Fig. 10(a) and (b) shows the measured and simulation results of the VP and HP elements without a feeding network. As shown in Fig. 10(a), the simulated 10 dB impedance bandwidth of the VP element is from 1.6 to 2.6 GHz and from 1.65 to 2.5 GHz for the measured one. The corresponding fractional bandwidths are about 47.6% and 41%, respectively. Fig. 10(b) presents the impedance bandwidth of the HP element ($|S_{22}|$ and $|S_{33}| < -10$ dB) which is from 1.64 to 2.5 GHz for $|S_{22}|$ and 1.56 to 2.6 GHz for $|S_{33}|$ from the simulation, whereas the measured bandwidth ($|S_{22}|$ and $|S_{33}| < -9.4$ dB) is from 1.6 to 2.5 GHz for $|S_{22}|$ and 1.52 to 2.6 GHz for $|S_{33}|$. The peak gain values of the antenna are also presented in Fig. 10(a) and (b), where it is seen that the proposed design has stable peak gain values over the frequency band.

In order to combine ports 2 and 3 to achieve an HP omnidirectional radiation pattern, the HP element is fed by a broadband feeding network which consists of a power divider and a 90° phase shifter [19], as shown in Fig. 11(a). The return loss of the power divider and phase shifter is about 10 dB and the phase deviation of the phase shifter is within 6°. The measured results agree well with the simulated ones within the desired band. Fig. 11(b) demonstrates the measured S-parameters of the proposed dual-polarized antenna with the feeding network. It is clear that the proposed antenna achieves a wide bandwidth, which is from 1.65 to 2.5 GHz for the VP element and 1.5 to 2.47 GHz for the HP element. The measured S-parameter of the HP element is a little higher than

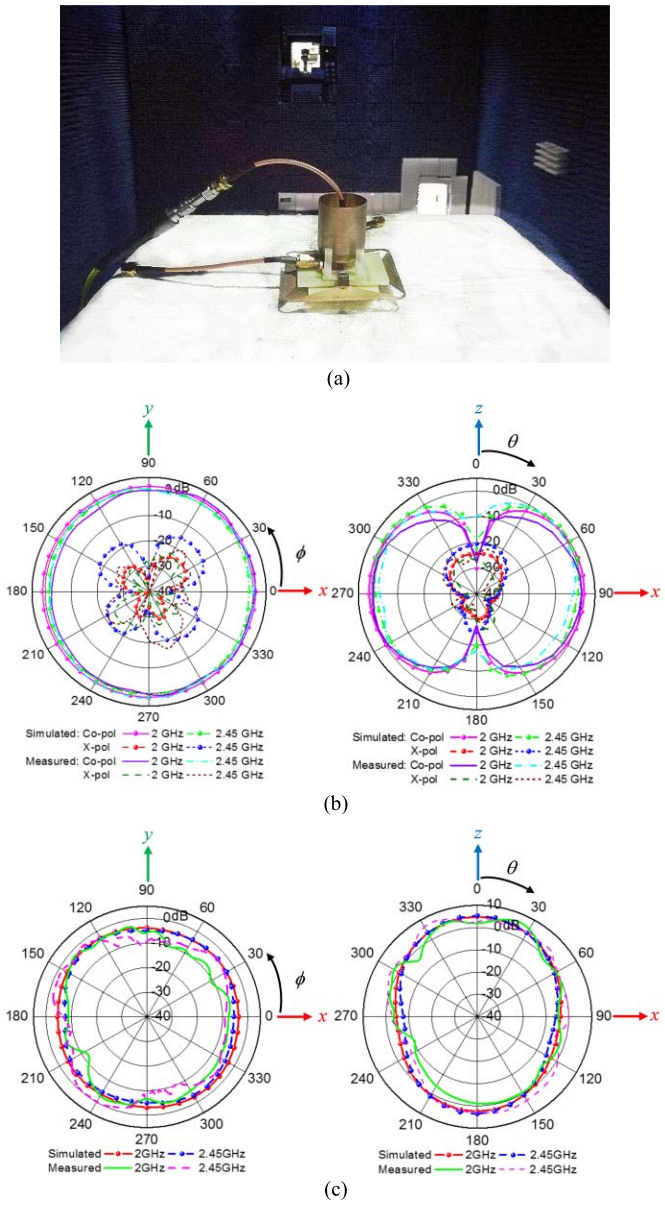

Fig. 12. (a) Measured environment of the proposed antenna and simulated and measured radiation patterns of (b) VP element and (c) HP element.

−10 dB, which is caused by the SMA connector and the balun. The isolation between the VP and HP ports is at least 25 dB. In addition, the measurement environment of the proposed antenna is presented in Fig. 12(a). The measured and simulated radiation patterns of the dual-polarized antenna are shown in Fig. 12(b) and (c), which exhibit good omnidirectional radiation patterns for both VP and HP.

It should be noted that the peak gain and radiation pattern of the HP element were not measured directly as the standard circularly polarized horn antenna was not available for the measurement system used. Instead, two linear polarization components of the modified cross bow-tie dipole were measured to synthesize the radiation pattern with the assumption of a 90° phase difference for the two ports. As such, the effects of the shorting pins could not be considered in the synthesized radiation pattern.

VI. Conclusion

A wideband omnidirectional antenna was presented to achieve dual polarizations. The proposed antenna integrates the VP and HP elements by adding a small circular ground for antenna miniaturization. The radiating mechanism of the proposed wideband dual-polarized omnidirectional antenna was analyzed and a parametric study was conducted to examine the influences of the phase difference on the antenna's radiation performance. In addition, the measured results are in good agreement with the simulated ones, which illustrates that the proposed design has achieved a high isolation, a wide bandwidth, and dual polarizations.

References

[1] H. Chreim, E. Pointereau, B. Jecko, and P. Dufrane, "Omnidirectional electromagnetic band gap antenna for base station applications," *IEEE Antennas Wireless Propag. Lett.*, vol. 6, pp. 499–502, 2007.

[2] B. Wang, F.-S. Zhang, L. Jiang, Q. Li, and J. Ren, "A broadband omnidirectional antenna array for base station," *Prog. Electromagn. Res.*, vol. 54, pp. 95–101, 2014.

[3] C.-C. Lin, L.-C. Kuo, and H.-R. Chuang, "A horizontally polarized omnidirectional printed antenna for WLAN applications," *IEEE Trans. Antennas Propag.*, vol. 54, no. 11, pp. 3551–3556, Nov. 2006.

[4] A. Elsherbini and K. Sarabandi, "Dual-polarized coupled sectorial loop antennas for UWB applications," *IEEE Antennas Wireless Propag. Lett.*, vol. 10, pp. 75–78, 2011.

[5] T. J. Judasz and B. B. Balsley, "Improved theoretical and experimental models for the coaxial colinear antenna," *IEEE Trans. Antennas Propag.*, vol. 37, no. 3, pp. 289–296, Mar. 1989.

[6] J. Zhao, D. Psychoudakis, C.-C. Chen, and J. L. Volakis, "Design optimization of a low-profile UWB body-of-revolution monopole antenna," *IEEE Trans. Antennas Propag.*, vol. 60, no. 12, pp. 5578–5586, Dec. 2012.

[7] X. Cai and K. Sarabandi, "A compact broadband horizontally polarized omnidirectional antenna using planar folded dipole elements," *IEEE Trans. Antennas Propag.*, vol. 64, no. 2, pp. 414–422, Feb. 2016.

[8] Y. Li, Z. Zhang, J. Zheng, and Z. Feng, "Compact azimuthal omnidirectional dual-polarized antenna using highly isolated colocated slots," *IEEE Trans. Antennas Propag.*, vol. 60, no. 9, pp. 4037–4045, Sep. 2012.

[9] E. A. Soliman, M. S. Ibrahim, and A. K. Abdelmageed, "Dual-polarized omnidirectional planar slot antenna for WLAN applications," *IEEE Trans. Antennas Propag.*, vol. 53, no. 9, pp. 3093–3097, Sep. 2005.

[10] C. Deng, P. Li, and W. Cao, "A high-isolation dual-polarization patch antenna with omnidirectional radiation patterns," *IEEE Antennas Wireless Propag. Lett.*, vol. 11, pp. 1273–1276, 2012.

[11] X.-W. Dai, Z.-Y. Wang, C.-H. Liang, X. Chen, and L.-T. Wang, "Multiband and dual-polarized omnidirectional antenna for 2G/3G/LTE application," *IEEE Antennas Wireless Propag. Lett.*, vol. 12, pp. 1492–1495, 2013.

[12] X. Quan and R. Li, "A broadband dual-polarized omnidirectional antenna for base stations," *IEEE Trans. Antennas Propag.*, vol. 61, no. 2, pp. 943–947, Feb. 2013.

[13] Y. Fan, X. Liu, B. Liu, and R. Li, "A broadband dual-polarized omnidirectional antenna based on orthogonal dipoles," *IEEE Antennas Wireless Propag. Lett.*, vol. 15, pp. 1257–1260, 2016.

[14] H. Huang, Y. Liu, and S. Gong, "Broadband dual-polarized omnidirectional antenna for 2G/3G/LTE/WiFi applications," *IEEE Antennas Wireless Propag. Lett.*, vol. 15, pp. 576–579, 2016.

[15] J. Wu, S. Yang, Y. Chen, S. W. Qu, and Z. Nie, "A low profile dual-polarized wideband omnidirectional antenna based on AMC reflector," *IEEE Trans. Antennas Propag.*, vol. 65, no. 1, pp. 368–374, Jan. 2017.

[16] J. Wang, Z. Shen, and L. Zhao, "Wideband dual-polarized antenna for spectrum monitoring systems," *IEEE Antennas Wireless Propag. Lett.*, vol. 16, pp. 2236–2239, 2017.

[17] K. Wei, Z. Zhang, Z. Feng, and M. F. Iskander, "Periodic leaky-wave antenna array with horizontally polarized omnidirectional pattern," *IEEE Trans. Antennas Propag.*, vol. 60, no. 7, pp. 3165–3173, Jul. 2012.

[18] C. A. Balanis, *Antenna Theory: Analysis and Design*, 3rd ed. Hoboken, NJ, USA: Wiley, 2005.

[19] J. Wang, Z. Shen, and L. Zhao, "UWB 90° phase shifter based on broadside coupler and T-shaped stub," *Electron. Lett.*, vol. 52, no. 25, pp. 2048–2050, Dec. 2016.

Jun Wang was born in Jiangsu, China. He received the B.Eng. and M.S. degrees from Jiangsu Normal University, Xuzhou, China, in 2013 and 2017, respectively. He is currently pursuing the Ph.D. degree in Southeast University, Nanjing, China.

His current research interests include the design of RF/microwave antennas and phase shifter.

Lei Zhao (M'09) received the B.S. degree in mathematics from Jiangsu Normal University, Xuzhou, China, 1997, and the M.S. degree in computational mathematics and the Ph.D. degree in electromagnetic fields and microwave technology from Southeast University, Nanjing, China, in 2004 and 2007, respectively.

From 2007 to 2009, he was a Research Associate with the Department of Electronics Engineering, The Chinese University of Hong Kong, Hong Kong. In 2009, he joined Jiangsu Normal University, as an Assistant Professor, and was promoted to an Associate Professor in 2012. In 2011, he joined the Department of Electronics and Computer Engineering, National University of Singapore, Singapore, as a Research Fellow. He is currently the Associate Director with the Jiangsu Key Laboratory of Education Big-Data Science and Engineering, Xuzhou, China, and the Vice Dean with the School of Mathematics and Statistics, Xuzhou, China. He has authored or co-authored over 40 refereed journal and conference papers. His current research interests include computational electromagnetics, bioelectromagnetics, and millimeter-wave components, including filters and antenna arrays.

Zhang-Cheng Hao (M'08–SM'15) received the B.S. degree in microwave engineering from Xidian University, Xi'an, China, in 1997, and the M.S. degree and the Ph.D. degree in radio engineering from Southeast University, Nanjing, China, in 2002 and 2006, respectively.

In 2006, he joined the Laboratory of Electronics and Systems for Telecommunications, École Nationale Supérieure des Télécommunications de Bretagne, Brest, France, as a Post-Doctoral Researcher, where he was involved in the development of millimeter-wave antennas. In 2007, he joined the Department of Electrical, Electronic and Computer Engineering, Heriot-Watt University, Edinburgh, U.K., as a Research Associate, where he was involved in the development of multilayer integrated circuits and ultra-wideband components. In 2011, he joined the School of Information Science and Engineering, Southeast University, Nanjing, China, as a Professor. He has authored or co-authored over 150 referred journal and conference papers and holds 20 granted patents. His current research interests include microwave and millimeter-wave systems, submillimeter-wave and terahertz components, and passive circuits, including filters, antenna arrays, couplers, and multiplexers.

Dr. Hao was a recipient of the Thousands of Young Talents presented by China Government in 2011 and the High Level Innovative and Entrepreneurial Talent presented by Jiangsu Province, China, in 2012. He has served as a reviewer for many technical journals, including the IEEE TRANSACTIONS ON MTT, the IEEE TRANSACTIONS ON AP, the IEEE AWPL, and the IEEE MWCL.

Jian-Ming Jin (S'87–M'89–SM'94–F'01) received the Ph.D. degree in electrical engineering from the University of Michigan, Ann Arbor, MI, USA, in 1989.

In 1993, he joined the University of Illinois at Urbana–Champaign, Urbana, IL, USA, where he is currently the Y. T. Lo Chair Professor of electrical and computer engineering and the Director of the Electromagnetics Laboratory and Center for Computational Electromagnetics. He has authored or co-authored over 250 papers in refereed journals and 22 book chapters. He has also authored *The Finite Element Method in Electromagnetics* (Wiley, first edition 1993, second edition 2002, and third edition 2014), the *Electromagnetic Analysis and Design in Magnetic Resonance Imaging* (CRC, 1998), and the *Theory and Computation of Electromagnetic Fields* (Wiley, first edition 2010 and second edition 2015), and has co-authored the *Computation of Special Functions* (Wiley, 1996), the *Fast and Efficient Algorithms in Computational Electromagnetics* (Artech, 2001), and *Finite Element Analysis of Antennas and Arrays* (Wiley, 2008). His current research interests include computational electromagnetics, scattering and antenna analysis, electromagnetic compatibility, high-frequency circuit modeling and analysis, bioelectromagnetics, and magnetic resonance imaging. He was elected by ISI as one of the world's most cited authors in 2002.

Dr. Jin is a Fellow of the Electromagnetics Academy and Applied Computational Electromagnetics Society (ACES), and a member of URSI Commission B. He was a recipient of the 1994 National Science Foundation Young Investigator Award, the 1995 Office of Naval Research Young Investigator Award, the 1999 ACES Valued Service Award, the 2014 ACES Technical Achievement Award, the 2016 ACES Computational Electromagnetics Award, the 2015 IEEE Antennas and Propagation Society Chen-To Tai Distinguished Educator Award, and the 2015 IEEE Antennas and Propagation Edward E. Altschuler AP-S Magazine Prize Paper Award. He also received the 1997 Xerox Junior Research Award and the 2000 Xerox Senior Research Award presented by the College of Engineering, University of Illinois at Urbana–Champaign, and was appointed as the first Henry Magnuski Outstanding Young Scholar in the Department of Electrical and Computer Engineering in 1998, and later as a Sony Scholar in 2005. He was appointed as a Distinguished Visiting Professor in the Air Force Research Laboratory in 1999 and was awarded Adjunct, Visiting, Guest, or Chair Professorship by 11 institutions around the world. His name appeared 22 times in the University of Illinois at Urbana–Champaign's List of Excellent Instructors. His students have won the best paper awards in the IEEE 16th Topical Meeting on Electrical Performance of Electronic Packaging and 25th, 27th, 31st, and 32nd Annual Review of Progress in Applied Computational Electromagnetics. He served as an Associate Editor and a Guest Editor of the IEEE TRANSACTIONS ON ANTENNAS AND PROPAGATION, *Radio Science, Electromagnetics*, *Microwave and Optical Technology Letters*, and *Medical Physics*.